



## Improving the determination of the gravity rate of change by combining superconducting with absolute gravimeter data

Michel J. Van Camp<sup>a,b,\*</sup>, Olivier de Viron<sup>b</sup>, Richard J. Warburton<sup>c</sup>

<sup>a</sup> Royal Observatory of Belgium, Avenue Circulaire 3, BE-1180 Brussels, Belgium

<sup>b</sup> Univ. Paris Diderot, Sorbonne Paris Cité, Institut de Physique du Globe de Paris, F-75013 Paris, France

<sup>c</sup> GWR Instruments Inc, 6264 Ferris Square, Suite D, San Diego, CA 92121, USA

### ARTICLE INFO

#### Article history:

Received 31 May 2012

Received in revised form

24 July 2012

Accepted 25 July 2012

Available online 4 August 2012

#### Keywords:

Superconducting gravimeter

Absolute gravimeter

Gravity rate of change

Slow tectonic deformations

Environmental effects

Least squares fitting

### ABSTRACT

This paper evaluates different data-processing methods to determine the gravity rate of change, using repeated absolute gravimeter (AG) measurements and continuous monitoring by a superconducting gravimeter (SG). Based on synthetic data representative of signals observed by SGs at various station locations, we demonstrate that the addition of SG information mitigates the error in the estimation of gravity rates of change caused by the presence of long period, interannual, and annual signals in the AG data. These results are discussed as a function of the sampling rate of the absolute gravity measurements, the duration of the observations, and the uncertainties of the AGs.

© 2012 Elsevier Ltd. All rights reserved.

### 1. Introduction

Monitoring long-term vertical ground motion is mandatory in many studies involving tectonics or glacial isostatic adjustment. This task is challenging as the signals from ground motion are at the limit of the uncertainty of current geodetic techniques and may be obscured by other larger signals of geophysical origin. Deformation studies traditionally use Global Navigation Satellite System (GNSS), but reference-frame issues make it much less reliable in monitoring the long-term vertical displacement (Mazzotti et al., 2007; Van Camp et al., 2011). Gravity studies of vertical deformation have generally been the exclusive domain of absolute gravimeters (AGs). AGs have two paramount advantages over relative gravity meters: They have no long-term instrumental drift and, as a standard, they can determine the gravity at any location to a known accuracy. However, for both logistical reasons and mechanical degradation, AGs are not normally used for continuous monitoring of a station, but rather they are used to visit a given network station either one time or a few times per year. This can lead to aliasing caused by hydrology or other sources that are not precisely determined in the absence of continuous measurements.

Although SGs are about 100 times more precise than AGs (Van Camp et al., 2005), they typically exhibit small linear drifts, of order  $2 \mu\text{Gal}/\text{year}$  ( $1 \mu\text{Gal} = 10 \text{ nm s}^{-2}$ ), the order of the investigated signals or larger. Although Van Camp and Francis (2006) have measured an exponential drift on the SG operating at Membach, Belgium, no other examples of such long-term non-linear drift have been reported for other SGs. At typical SG sites, such as GGP stations (Crossley and Hinderer, 2008), AGs visit SG stations on a quasi-regular basis to determine the SG drift. AGs are also operated next to the SG for several days to determine its calibration factor (Francis et al., 1998). Depending on the SG station, the repetition rate of the AG measurements varies: It can be a few weeks (Weise et al., 2009), one month (Van Camp et al., 2005; Longuevergne et al., 2008; Palinkas et al., 2010), one time to a few times per year (Van Camp et al., 2011; Creutzfeldt et al., 2010; Zerbini et al., 2007), or even less (Mémin et al., 2011; Omang and Kierulf, 2011).

These drifts prevent SGs from measuring deformation; however, Wziontek et al. (2008) show that the combination of AGs and SGs improves the precision of the gravity monitoring, e.g., by adjusting the differences in the absolute value measured with different AGs and detecting offsets in the AG data that may occur after repair or mishandling.

In this paper, we discuss how the information of the SG can be used together with the repeated AG measurements to best determine the gravity rate of change. This problem can be seen as follows: We have two independent measurements of the time

\* Corresponding author at: Royal Observatory of Belgium, Avenue Circulaire 3, BE-1180 Brussels, Belgium. Tel.: +32 2 373 0265; fax: +32 2 373 0339.

E-mail addresses: [mvc@oma.be](mailto:mvc@oma.be), [michel.vancamp@oma.be](mailto:michel.vancamp@oma.be) (M.J. Van Camp), [deviron@ippg.fr](mailto:deviron@ippg.fr) (O. de Viron), [warburton@gwrinstruments.com](mailto:warburton@gwrinstruments.com) (R.J. Warburton).

variable gravity. One (AG) is less precise and sparse, which can induce aliasing effects; the other (SG) is very precise and continuous, but with a small instrumental drift. Combining these data, we want to get the most precise estimation of the geophysical gravity rate of change. Many papers discussing slow trends at stations benefiting from both AG and SG instruments make use of the AG data only. This is the case of [Sato et al. \(2006\)](#) and [Mémin et al. \(2011\)](#), who analyze the gravity rate of change at Ny-Ålesund, Svalbard archipelago. Later on, [Omang and Kierulf \(2011\)](#) made use of the SG data at Ny-Ålesund, but they did not continue to discuss strategies of analysis. In this paper, we show how incorporating the SG data significantly improves the determination of the gravity rate of change.

## 2. Estimation methods

Let us suppose that, for a given station, we have two datasets:  $SG(t_i)$ , from the superconducting gravimeter, and  $AG(\tau_k)$ , from the absolute gravimeter. The AG dataset is sparse, with a few points per year. The SG data set, originally with a one-second sampling rate, has been averaged to daily values, as we are looking for a long-term signal.

### 2.1. Method 1: Simply fit the trend on the AG data

The SG data is not used in the analysis for this method; the geophysical trend  $\alpha$  is estimated from a linear fit on the time series  $AG(\tau_k)$ :

$$AG(\tau_k) = \alpha\tau_k + \beta \quad (1)$$

No attempt is made to estimate the seasonal signals, but measurements can be scheduled at the same time each year to minimize their impact.

For example, [Mémin et al. \(2011\)](#) use this method at Ny-Ålesund (Spitsbergen).

### 2.2. Method 2: Fit the trend and an annual wave on the AG data

As an annual signal is likely to be present, it is useful to fit an annual cycle together with the trend. To be thorough, the seasonal cycle should be composed of an annual and a semi-annual signal, which should both be determined. Since the semi-annual signal causes exactly the same aliasing problems as the annual signal, we chose to simplify the discussion by including only the annual term in the model. The fit model reads as follow:

$$AG(\tau_k) = \alpha\tau_k + \beta + \gamma\sin(\omega\tau_k) + \delta\cos(\omega\tau_k) \quad (2)$$

Even with yearly (or less frequent) data, modeling the annual term makes sense, since small deviations of the measurement epoch can generate a non-negligible error on the trend, especially for short time series.

This method is used, for example, by [Van Camp et al. \(2011\)](#).

### 2.3. Method 3: Use the SG data to estimate and remove the climate signal from the AG

First, this method estimates the instrumental drift and geophysical trend in the SG series by fitting a linear drift and an annual wave, and subtracts the linear part of the model from the SG data. Then, the corrected SG data  $SG_c(\tau_k)$  at the AG measurement epochs  $\tau_k$  are subtracted from the AG data  $AG(\tau_k)$ :

$$SG(t_i) = \zeta t_i + \chi + \gamma\sin(\omega t_i) + \delta\cos(\omega t_i) \quad (3)$$

$$SG_c(t_i) = SG(t_i) - (\zeta t_i + \chi) \quad (4)$$

$$AG_c(\tau_k) = AG(\tau_k) - SG_c(\tau_k) \quad (5)$$

If the SG drift is perfectly linear, this provides an essentially “climatic-free” AG series, apart from a possible contribution from slow climate changes to the trend. However, any deviation of the SG drift from linearity will contaminate the climate signal. Therefore, for this method to work well, it is extremely important that any deviation of the SG drift from linearity be very small compared to seasonal variations. Nevertheless, as our test focuses on the trend estimates, a contamination of the climate signal is unlikely to affect the trend estimate to a significant extent. Finally, the trend is estimated by fitting a degree-one polynomial on the corrected AG data:

$$AG_c(\tau_k) = \alpha\tau_k + \beta \quad (6)$$

As far as we know, this method has never been used.

### 2.4. Method 4: Correct the SG for its drift by using the AG data and estimate the gravity rate of change from the drift-corrected SG

In this method, the trend  $\alpha$  is determined from the drift-corrected SG time series  $SG_c(t_i)$ . The drift is estimated from the difference between AG and SG data at the common points  $\tau_k$ . For instance, for a linear drift, the model is:

$$SG(\tau_k) - AG(\tau_k) = \zeta\tau_k + \chi \quad (7)$$

Eq. (7) assumes that the AG measurements are perfect and allows the removal of common geophysical noise. The drift-corrected SG time series is:

$$SG_c(t_i) = SG(t_i) - (\zeta t_i + \chi) \quad (8)$$

The gravity rate of change  $\alpha$  is then estimated by fitting

$$SG_c(t_i) = \alpha t_i + \beta + \gamma\sin(\omega t_i) + \delta\cos(\omega t_i) \quad (9)$$

[Omang and Kierulf \(2011\)](#) use this method but do not account for the seasonal term.

### 2.5. Method 5: Global least square solution using the SG and AG data

Here, we directly perform a global fit on both the SG and AG time series. The model reads as follow:

$$AG(\tau_k) = \alpha\tau_k + \beta + \gamma\sin(\omega\tau_k) + \delta\cos(\omega\tau_k) \quad (10)$$

$$SG(t_i) = \alpha t_i + \zeta t_i + \mu + \gamma\sin(\omega t_i) + \delta\cos(\omega t_i) \quad (11)$$

As with Method 3, this has never been used.

## 3. Numerical simulation

In order to make a valid assessment of the precision of the trend as estimated by each method, we need to know exactly what the value of the trend is, and to dispose of datasets with the observation strategy required for our tests. Consequently, we made the assessment on synthetic data sets based on four typical situations, as determined by the amplitude of the seasonal and interannual signals.

The synthetic gravity signal, which does not include the atmospheric and Earth-tide signals, is composed of a seasonal signal with a random phase, white and red noise, an interannual variability, and a trend of 0.5  $\mu\text{Gal}/\text{yr}$  ([Fig. 1](#)). For the interannual variability, which is associated with climate dynamics – mostly of hydrological origin (see [Van Camp et al., 2010](#)) – we used a randomly chosen 30-year period of the North Atlantic Oscillation (NAO) index ([Hurrell, 1995](#)) ([Fig. 2a](#)).

The white noise is distributed as a Gaussian random variable with a zero mean and 1  $\mu\text{Gal}$  standard deviation, and the order

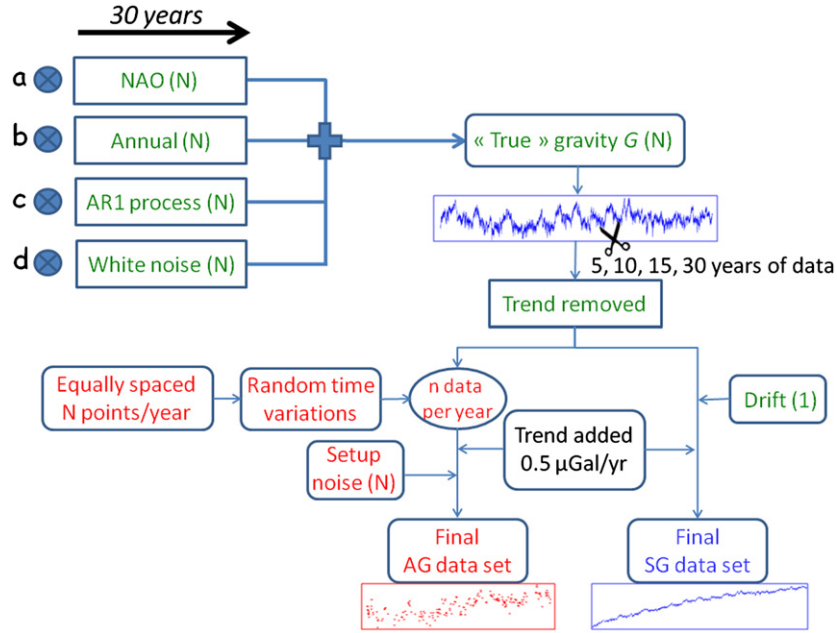


**Fig. 1.** Synthetic data production scheme. The drift is common for all the simulations (1 time series), whereas the North Atlantic Oscillation (NAO) index (Hurrell, 1995), annual term, degree one autoregressive AR1 noise, white noise, and setup noise are generated again using the same parameters (except for the starting date for the NAO selection) for each of the  $N=100,000$  simulations ( $N$  time series or phases).

one autoregressive red (AR1) noise is defined as:

$$x_{i+1} = \alpha x_i + z_i \quad (12)$$

where  $\alpha$  is the autocorrelation at lag 1 day ( $\alpha=0.016$ ) and  $z_i$  is a source term with a centered Gaussian distribution of standard deviation 0.2. The synthetic signal is corrected for any unknown trend resulting from the NAO or the noise before adding a  $0.5 \mu\text{Gal/yr}$  trend.

To generate the synthetic AG measurements, the gravity signal  $G(t)$  has been decimated. An initial time  $\tau_1$  has been chosen randomly within the first month of the  $G(t)$  series, and the other AG measurements times ( $\tau_i$ ) are regularly spaced with respect to the first one, along the whole length of the signal. Then, a positive or a negative random delay  $r_i$  shorter than 1 month has been added to each  $\tau_i$  measurement time. This is done to mimic actual campaigns, which usually cannot be repeated exactly at the same time each year. The AG signal is then obtained as the gravity signal  $G(\tau_i)$  at those times, to which a random noise  $w_i$  is added to account for the AG setup noise. Its standard deviation is  $1.6 \mu\text{Gal}$  according to Van Camp et al. (2005):

$$AG(\tau_i) = G(\tau_i) + w_i \quad (13)$$

with

$$\tau_i = \tau_1 + i\Delta\tau + r_i \quad (14)$$

where  $i$  is an integer (e.g., it corresponds to 12 months when simulating yearly AG campaigns) and  $r_i$ , the random delay. For the SG, a linear drift  $B=2 \mu\text{Gal/year}$  is added to the gravity time series:

$$SG(t) = G(t) + Bt \quad (15)$$

The SG random noise has been disregarded in this study, since it has a standard deviation 100 times smaller than that of the AG.

All together, the simulated run is determined by three parameters: the amplitude of the NAO, the amplitude of the annual, and the amplitude of the AG setup noise, parameterized by its standard deviation. In what follows, we will refer to each experiment by a 3 sign code. The first one with a capital letter for the scale of the NAO signal ( $A=2$ ,  $B=4$ ), the second one with a

lowercase letter for the amplitude of the annual signal ( $a=1$ ,  $b=2$ ,  $c=10$ ), and the dispersion of the AG setup noise represented by its standard deviation. It amounts to  $1.6 \mu\text{Gal}$  or  $4.0 \mu\text{Gal}$  if more than one AG is used and if the gravimeters are not intercompared. In that case,  $4.0 \mu\text{Gal}$  is taken as the higher limit of the AG differences evidenced for the last international comparisons of absolute gravimeters (e.g., de Viron et al., 2011). Such a high setup value may also be considered when only one AG is used, if the instrument is not correctly maintained and never compared against other AGs or an SG at a reference station.

The five experiments are summarized in Table 1 and illustrated on Fig. 2b–f; they are chosen from the different types of behavior of the SG time series discussed in Van Camp et al. (2010). These synthetic cases are not exhaustive, but they are sufficient to test and compare the performance of the different methods of processing the data, which is the main goal of this paper. The five methods are tested for 5, 10, 15 and 30-year long time series for AG measurements occurring 1, 2, and 4 times per year or less than once a year (i.e., once a year but with 1, 2 or 4 data points missing). We then generated 100,000 time series with the parameters defined above.

## 4. Simulation results

### 4.1. Performance of the different methods

From the 100,000 simulations for each case, we obtained 100,000 trend estimations for each method. Fig. 3 summarizes the results for the case Ac1.6; each subpanel represents, for the five methods, the histogram of the retrieved trends for a given data length (e.g., 5 years) and sampling rate (e.g., 1 point per year). For all cases, the numerical values of the standard deviations are given in Table 2, for one AG measurement per year.

As expected from the zero trend imposed on the combination of all the noise sources, the estimation methods are found unbiased. The methods differ significantly by their dispersions: The least dispersed are the most reliable as they are less likely to leave an erroneous trend estimate. Not surprisingly, for a given

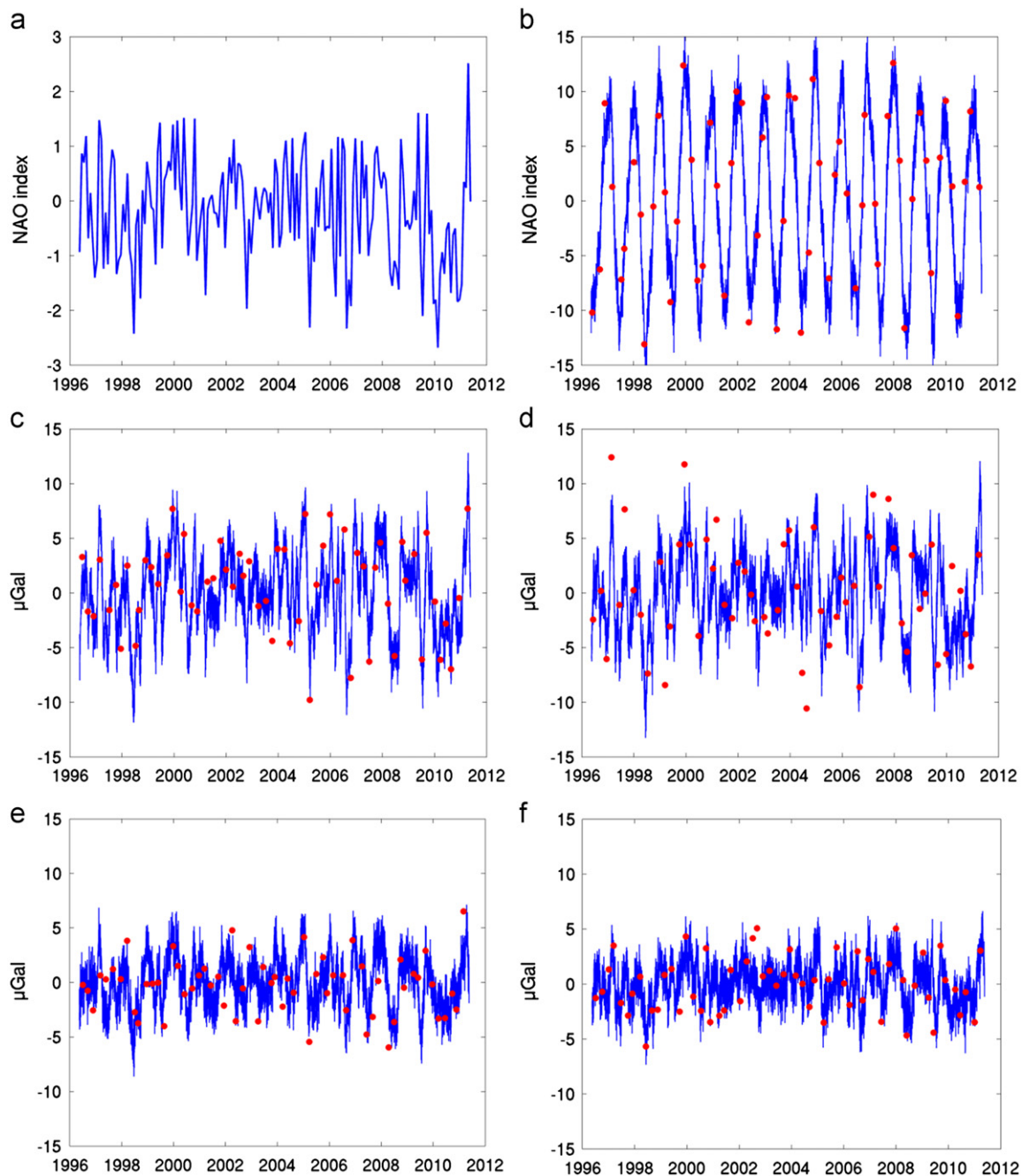


**Fig. 2.** (a): time series of the North Atlantic Oscillation (NAO) index. (b–f): Simulated SG (blue) and AG (red dots) time series, obtained by adding the North Atlantic Oscillation (NAO), an annual term, a degree one autoregressive red noise (amplitude  $2 \mu\text{Gal}$ , autocorrelation  $0.4/h$ , innovation parameter  $0.2$ ), a white noise (amplitude  $1 \mu\text{Gal}$ ), and a geophysical trend of  $0.5 \mu\text{Gal}/\text{yr}$ . The AG series (here 4 per year) also includes a setup noise of  $1.6 \mu\text{Gal}$  or  $4.0 \mu\text{Gal}$  (see Table 1). For clarity the SG drift and the geophysical trend are set to 0. (b) Case Aa: amplitude NAO:  $2 \mu\text{Gal}$ , annual signal:  $10 \mu\text{Gal}$ ; (c) case Bb: Amplitude NAO:  $4 \mu\text{Gal}$ , annual signal:  $2 \mu\text{Gal}$ ; (d) same as (c) but for an AG setup noise of  $4 \mu\text{Gal}$ ; (e) case Ab: amplitude NAO:  $2 \mu\text{Gal}$ , annual signal:  $2 \mu\text{Gal}$ ; (f) case Aa: amplitude NAO:  $2 \mu\text{Gal}$ , annual signal:  $1 \mu\text{Gal}$ . These 5 cases are summarized in Table 1. (For interpretation of the references to color in this figure legend, the reader is referred to the web version of this article.)

sampling rate, AG setup noise, and case, the longer the time series, the smaller the dispersion of the estimator (Figs. 3 and 4).

Method 1 and 2 show the worst performances, which makes sense as they use less information than the other three. One may expect Method 2 to perform much better than Method 1, as the model is better. But this is actually only the case when the annual signal is strong (case Aa1.6) or when enough data, i.e., at least 4 points a year, are available; otherwise, fitting the annual signal makes things worse (Fig. 4). More unexpected is the poor performance of Method 5, which makes a general inversion of the problem compared to Methods 3 and 4, which investigate the

SG and AG data separately. This can be explained by the fact that the global inversion requires a full model of the problem, i.e., a model that includes the interannual component of the signal, and this is not possible unless the interannual behavior is known. On the other hand, Methods 3 and 4, based on differences between the AG and SG, allow for correcting the unknown interannual signal. Method 4 gives better results than Method 3 for two reasons: (1) it estimates the SG drift using the differences between SG and AG at the AG points, so that no interannual signal remains in the drift estimation; (2) it estimates the trend using significantly more data (based on the SG points) than

Method 3 does (based on the AG points). The first reason is most likely the most significant, as one does not need that many points to get a robust trend estimate.

Table 3 shows that the trend determined by Method 4 can be up to 66% better, i.e., the standard deviation of the estimator is 66% smaller than that determined by Method 1. When the AG setup noise amounts to 4.0  $\mu\text{Gal}$ , the improvement is still observed at the level of 7–30%, except for measurements performed for only 5 years. Under such circumstances a decrease is observed for the Bb case if less than one AG measurement is performed each year, and for the other cases, if 4 AG data points are available each year. This shows that taking too many poor AG measurements can decrease the quality of the trend estimate when the interannual geophysical signal is weak (cases Aa, Ab and Ac).

4.2. Influence of the AG campaign rate and setup noise

We now focus on Method 4, which has been shown to be the best. Considering that only the AG setup noise affects the drift determination of Method 4, which induces the corresponding error on the trend determination, it is possible to compute analytically the expected error standard deviation for Method 4 if we neglect the impact of the random fluctuation of the AG sampling. Note that the setup noise is known to be normally

distributed (Van Camp et al., 2005; Palinkas et al., 2010). For uncorrelated error on the observation, the variance–covariance matrix of the retrieved parameters is given by Freedman (2005):

$$M = \sigma(A^T A)^{-1}$$

Applied to the trend estimate by Method 4, we obtain the standard deviation of the retrieved trend as:

$$\sigma_{\text{trend}} = \sigma/L(12/N)^{1/2},$$

with  $\sigma$ , the standard deviation of the data;  $L=N\Delta t$ , the time length of the dataset; and  $N$ , the number of observations.

To improve the trend determination, it is more useful to measure a long time ( $\sigma_{\text{trend}}$  decreases as  $1/L$ ), than to have a large number of measurements ( $\sigma_{\text{trend}}$  decreases as  $1/N^{1/2}$ ): e.g., it is more rewarding to measure once a year during 15 years than make 4 measurements a year for 5 years.

Table 2

Standard deviation of the trend recovered by applying each of the five methods, for one absolute gravity measurement performed each year, after 5/10/15/30 years. The bold values are for 15 years. The case Ac1.6 is illustrated in the middle column of Fig. 3.

	Years	Method 1	Method 2	Method 3	Method 4	Method 5
Ac1.6	5	1.07	2.29	1.65	0.81	0.83
	10	0.36	0.32	0.21	0.19	0.27
	15	<b>0.20</b>	<b>0.16</b>	<b>0.11</b>	<b>0.10</b>	<b>0.15</b>
	30	0.08	0.06	0.04	0.03	0.06
Bb1.6	5	1.27	3.49	1.65	0.82	1.26
	10	0.39	0.48	0.22	0.19	0.39
	15	<b>0.22</b>	<b>0.24</b>	<b>0.11</b>	<b>0.10</b>	<b>0.22</b>
	30	0.10/	0.10	0.04	0.03	0.10
Bb4.0	5	1.73	4.57	3.46	2.04	1.72
	10	0.56	0.68	0.53	0.48	0.56
	15	<b>0.31</b>	<b>0.34</b>	<b>0.26</b>	<b>0.25</b>	<b>0.31</b>
	30	0.13	0.13	0.09	0.09	0.12
Ab1.6	5	0.84	2.33	1.49	0.82	0.83
	10	0.27	0.33	0.21	0.19	0.27
	15	<b>0.15</b>	<b>0.16</b>	<b>0.11</b>	<b>0.10</b>	<b>0.15</b>
	30	0.06	0.06	0.04	0.03	0.06
Aa1.6	5	0.83	2.32	1.63	0.81	0.83
	10	0.27	0.33	0.21	0.19	0.27
	15	<b>0.15</b>	<b>0.16</b>	<b>0.11</b>	<b>0.10</b>	<b>0.15</b>
	30	0.06	0.06	0.04	0.03	0.06

Table 1

Case studies nomenclature as a function of the NAO and annual signal amplitude, and uncertainty on the repeated AG measurements. These cases are illustrated on Fig. 2 and the SG stations are characterized according to Van Camp et al. (2010).

Acronym	NAO amplitude [ $\mu\text{Gal}$ ]	Annual amplitude [ $\mu\text{Gal}$ ]	AG setup noise [ $\mu\text{Gal}$ ]	Example SG stations
Ac1.6	2 (A)	10 (c)	1.6	Tigo
Bb1.6	4 (B)	2 (b)	1.6	Ny-Ålesund, Cantley,
Bb4.0			4	Metsähovi
Ab1.6	2 (A)	2 (b)	1.6	Membach, Strasbourg, Bad Homburg
Aa1.6	2 (A)	1 (a)	1.6	Medicina, Vienna, Canberra, Moxa

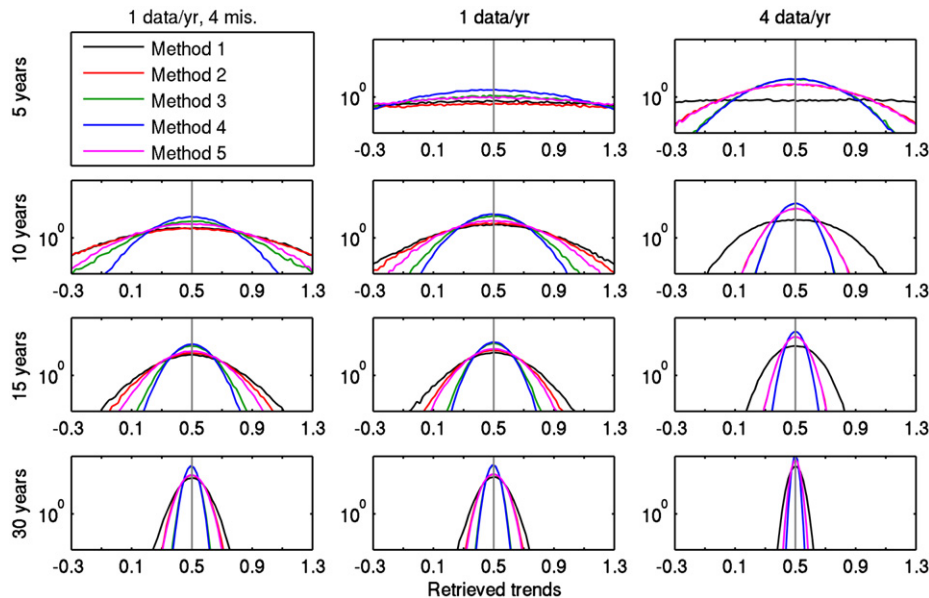
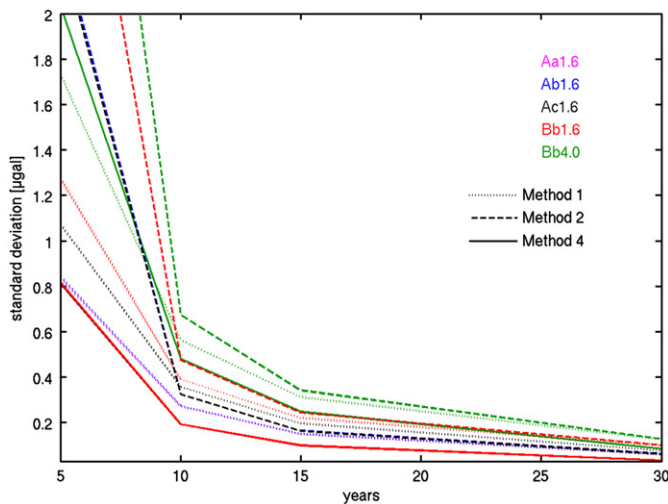


Fig. 3. Probability distribution (%) of the error on the trend (real value: 0.5  $\mu\text{Gal}/\text{yr}$ ), for the case Ac1.6, as a function of the five methods discussed in Section 2, and of the length of the time series (5, 10, 15 and 30 years) and the available absolute gravity measurements (once per year 4 missing, once a year and 4/year).



**Fig. 4.** Standard deviations of the retrieved trends for the Methods 1, 2, and 4 and all cases as a function of time, for an AG sampling rate of 1 data per year, as in Table 2. Methods 3 and 5 provide similar results as Method 4 and 2, respectively and are not shown for clarity. For Method 4 all the curves but the green one are superimposed.

**Table 3**

Difference in % between the standard deviations obtained by Method 1 and Method 4, taking 1, 2 and 4 AG data per year, after 5, 10, 15 and 30 years. The improvement is observed even for high setup noise, except for short and sparse AG datasets: A decrease in quality up to  $-18\%$  is observed for Bb4.0 when one or lesser AG measurements a year are performed for 5 years.

Years	Low setup noise 1.6 $\mu\text{Gal}$ Aa1.6, Ab1.6, Ac1.6, Bb1.6 (%)	High setup noise 4.0 $\mu\text{Gal}$ Aa4.0, Ab4.0, Ac4.0, Bb4.0 (%)
5	3–66	–19–35
10	29–62	7–29
15	30–59	7–25
30	33–66	7–25

A comparison with the simulated value shows that this explains more than 90% of the observed standard deviations, except for yearly (or less frequent) data for 5 years. The remaining discrepancies from this model are caused by the random fluctuation of the time sampling, which has more impact in the cases where little data is available.

If more than one AG is used, and if the gravimeters are not intercompared, the offsets between the instruments are unknown and the uncertainty on the AG measurements increases from 1.6  $\mu\text{Gal}$  to 4.0  $\mu\text{Gal}$ . For Method 4 the ratio between the standard deviation from the Bb4.0 and the Bb1.6 cases equals  $4/1.6=2.5$  (Table 2). The ratio is smaller for the other methods, as their uncertainty also includes other factors independent of the setup noise.

Adding AG data always provides an estimator of the trend with a smaller variance, but, as expected, this improvement decreases when the AG setup noise increases. In other words, we face a “garbage in, garbage out” situation (Butler et al., 2010).

## 5. Discussion and conclusions

In this paper, we test different methods for estimating a trend from the AG data using synthetic data. All the methods that include both the SG and AG series provide a better trend estimate, the best one being Method 4. The improvement brought by Method 5 is not significant, because the non-seasonal climate signal is not accounted for. We also study the impact of the length

and sampling of the time series, and we determine the precision of the estimator in each case. Due to the characteristics of the climate noise and to the fact that we determine the trend, it is more rewarding to measure for a long time than with a higher sampling. We also show that, for Method 4, the precision of the estimation is independent from the amplitude of the annual and interannual signals; only the AG setup noise impacts the quality of the estimator. Consequently, the use of more than one AG reduces the quality of the trend estimation, which becomes even more dramatic if the AGs are not properly intercompared.

This paper investigates a somewhat ideal situation, as we suppose that the SG only includes a stable drift and the climate signal and we remove any additional trends from the red noise or the climatic signal. In a real situation, the tectonic trend is mixed with a trend of climate origin; for example, if NAO is considered only between 1996 and 2011, a trend is found (Fig. 2a). This effect can be mitigated by using longer time series, which depend on the climatic context of the gravimeter, as shown by Van Camp et al. (2010). The present paper demonstrates that Method 4 is best to estimate the true trend in the gravity measurements, but it does not help for separating the tectonic trend signal from other origins. The development shown here could be used in other situations or instrumental setups, where the same quantity is monitored using two methods: one relative, very precise, and continuous, but with unknown stable drift, and one less precise and sparse, but absolute. In the case of spring gravimeters, however, the drifts are not as stable as the ones of SGs, especially for time series longer than a few months (Riccardi et al., 2011; Kang et al., 2011).

## Acknowledgements

Part of the work of MVC and the contribution of OdV is IGP contribution 3311. This work benefited from the support of the University Paris Diderot Space Campus, the Institut Universitaire de France and the Centre National d'Etudes Spatiales (CNES). We thank B. Meurers, two anonymous reviewers, and the Editor J. Caers for their assistance in evaluating this paper. We also appreciate the valuable advice from O. Francis and V. Mikhailov.

## References

- Butler, J., Lidwell, W., Holden, K., 2010. Universal Principles of Design: 125 Ways to Enhance Usability, Influence Perception, Increase Appeal, Make Better Design Decisions, and Teach Through Design. Rockport Publishers 272pp.
- Creutzfeldt, B., Guntner, A., Thoss, H., Merz, B., Wziontek, H., 2010. Measuring the effect of local water storage changes on in situ gravity observations: case study of the Geodetic Observatory Wettzell Germany. Water Resources Research 46, W08531, <http://dx.doi.org/10.1029/2009WR008359>.
- Crossley, D., Hinderer, J., 2008. A review of the GGP network and scientific challenges. Journal of Geodynamics 48, 299–304, <http://dx.doi.org/10.1016/j.jog.2009.09.019>.
- de Viron, O., Van Camp, M., Francis, O., 2011. Revisiting absolute gravimeter intercomparisons. Metrologia 48, 290–298, <http://dx.doi.org/10.1088/0026-1394/48/5/008>.
- Francis, O., Niebauer, T.M., Sasagawa, G., Klotting, F., Gschwind, J., 1998. Calibration of a superconducting gravimeter by comparison with an absolute gravimeter FG5 in Boulder. Geophysical Research Letters 25 (7), 1075–1078, <http://dx.doi.org/10.1029/98GL00712>.
- Freedman, D.A., 2005. Statistical Models: Theory and Practice. Cambridge University Press, New York, NY 414 pp.
- Hurrell, J.W., 1995. Decadal trends in the North Atlantic Oscillation and relationships to regional temperature and precipitation. Science 269, 676–679.
- Kang, K., Li, H., Peng, P., Hao, H., Wei, J., 2011. Seasonal variations in hydrological influences on gravity measurements using gPhones. Terrestrial Atmospheric and Oceanic Sciences 22 (2), 157–168, [http://dx.doi.org/10.3319/TAO.2010.08.02.01\(TibXS\)](http://dx.doi.org/10.3319/TAO.2010.08.02.01(TibXS)).
- Longuevergne, L., Boy, J.P., Florsch, N., Viville, D., Ferhat, G., Ulrich, P., Luck, B., Hinderer, J., 2008. Local and global hydrological contributions to gravity variations observed in Strasbourg. Journal of Geodynamics 48 (3–5), 189–194, <http://dx.doi.org/10.1016/j.jog.2009.09.008>.

- Mazzotti, S., Lambert, A., Courtier, N., Nykolaishen, L., Dragert, H., 2007. Crustal uplift and sea level rise in northern Cascadia from GPS, absolute gravity, and tide gauge data. *Geophysical Research Letters* 34, L15306, <http://dx.doi.org/10.1029/2007GL030283>.
- Mémin, A., Rogister, Y., Hinderer, J., Omang, O.C., Luck, B., 2011. Secular gravity variation at Svalbard (Norway) from ground observations and GRACE satellite data. *Geophysical Journal International* 184 (3), 1119–1130, <http://dx.doi.org/10.1111/j.1365-246X.2010.04922.x>.
- Omang, O.C.D., Kierulf, H.P., 2011. Past and presentday ice mass variation on Svalbard revealed by superconducting gravimeter and GPS measurements. *Geophysical Research Letters* 38, L22304, <http://dx.doi.org/10.1029/2011GL049266>.
- Palinkas, V., Kostecky, J., Simek, J., 2010. A feasibility of absolute gravity measurements in geodynamics. *Acta Geodynamica Geomateriala* 7 (1), 61–69. (157).
- Riccardi, U., Rosat, S., Hinderer, J., 2011. Comparison of the Micro-g LaCoste gPhone-054 spring gravimeter and the GWR-C026 superconducting gravimeter in Strasbourg (France) using a 300-day time series. *Metrologia* 48, 28–39, <http://dx.doi.org/10.1088/0026-1394/48/1/003>.
- Sato, T., Okuno, J., Hinderer, J., MacMillan, D.S., Plag, H.P., Francis, O., Falk, R., Fukuda, Y., 2006. A geophysical interpretation of the secular displacement and gravity rates observed at NyÅlesund, Svalbard in the Arctic—effects of postglacial rebound and presentday ice melting. *Geophysical Journal International* 165 (3), 729–743, <http://dx.doi.org/10.1111/j.1365-246X.2006.02992.x>.
- Van Camp, M., Williams, S.D.P., Francis, O., 2005. Uncertainty of absolute gravity measurements. *Journal of Geophysical Research* 110, B05406, <http://dx.doi.org/10.1029/2004JB003497>.
- Van Camp, M., Francis, O., 2006. Is the instrumental drift of superconducting gravimeters a linear or exponential function of time? *Journal of Geodesy* 81 (5), 337–344, <http://dx.doi.org/10.1007/s00190-006-0110-4>.
- Van Camp, M., Métivier, L., de Viron, O., Meurers, B., Williams, S.D.P., 2010. Characterizing long time scale hydrological effects on gravity for improved distinction of tectonic signals. *Journal of Geophysical Research* 115, B07407, <http://dx.doi.org/10.1029/2009JB006615>.
- Van Camp, M., de Viron, O., Scherneck, H.G., Hinzen, K.G., Williams, S.D.P., Lecocq, T., Quinif, Y., Camelbeeck, T., 2011. Repeated absolute gravity measurements for monitoring slow intraplate vertical deformation in western Europe. *Journal of Geophysical Research* 116, B08402, <http://dx.doi.org/10.1029/2010JB008174>.
- Weise, A., Kroner, C., Abe, M., Ihde, J., Jentzsch, G., Naujoks, M., Wilmes, H., Wziontek, H., 2009. Gravity field variations from superconducting gravimeters for GRACE validation. *Journal of Geodynamics* 48 (3-5), 325–330, <http://dx.doi.org/10.1016/j.jog.2009.09.034>.
- Wziontek, H., Falk, R., Wilmes, H., Wolf, P., 2008. Precise gravity time series and instrumental properties from combination of superconducting and absolute gravity measurements. In: Sideris, M.G. (Ed.), *International Association of Geodesy Symposia*, 133; 2008, pp. 301–306, [http://dx.doi.org/10.1007/978-3-540-85426-5\\_35](http://dx.doi.org/10.1007/978-3-540-85426-5_35).
- Zerbini, S., Richter, B., Rocca, F., van Dam, T., Matonti, F., 2007. A combination of space and terrestrial geodetic techniques to Monitor Land subsidence: case study, the Southeastern Po Plain, Italy. *Journal of Geophysical Research* 112, B05041, <http://dx.doi.org/10.1029/2006JB004338>.